

Discriminant Genetic Algorithm Extended (DGAE) model for seasonal sand and dust storm prediction

YANG YuanQin, WANG JiZhi*, HOU Qing, LI Yi & ZHOU ChunHong

Key Laboratory for Atmospheric Chemistry, Center for Atmospheric Watch and Services, Chinese Academy of Meteorological Sciences, China Meteorological Administration, Beijing 100081, China

Received January 29, 2010; accepted May 12, 2010; published online October 16, 2010

Here we use a Discriminant Genetic Algorithm Extended (DGAE) model to diagnose and predict seasonal sand and dust storm (SDS) activities occurring in Northeast Asia. The study employed the regular meteorological data, including surface data, upper air data, and NCEP reanalysis data, collected from 1980–2006. The regional, seasonal, and annual differences of 3-D atmospheric circulation structures and SDS activities in the context of spatial and temporal distributions were given. Genetic algorithms were introduced with the further extension of promoting SDS seasonal prediction from multi-level resolution. Genetic probability was used as a substitute for posterior probability of multi-level discriminants, to show the dual characteristics of crossover inheritance and mutation and to build a non-linear adaptability function in line with extended genetic algorithms. This has unveiled the spatial distribution of the maximum adaptability, allowing the forecast field to be defined by the population with the largest probability, and made discriminant genetic extension possible. In addition, the effort has led to the establishment of a regional model for predicting seasonal SDS activities in East Asia. The model was tested to predict the spring SDS activities occurring in North China from 2007 to 2009. The experimental forecast resulted in highly discriminant intensity ratings and regional distributions of SDS activities, which are a meaningful reference for seasonal SDS predictions in the future.

sand and dust storms, seasonal prediction methodology, Discriminant Genetic Algorithm Extended (DGAE) model

Citation: Yang Y Q, Wang J Z, Hou Q, et al. Discriminant Genetic Algorithm Extended (DGAE) model for seasonal sand and dust storm prediction. *Sci China Earth Sci*, 2011, 54: 10–18, doi: 10.1007/s11430-010-4059-z

A range of worldwide natural disasters, including droughts, desertification, floods, and damage from freezing conditions, have occurred in an increased frequency and enhanced intensity that threaten human safety and welfare. According to the United Nations Environment Program (UNEP), 35% of the world's land and 20% of the population are threatened by droughts and desertification. In China, two-thirds of the country is subject to torrential rains, floods, droughts and desertification [1]. A study by Li [2] pointed out that in densely populated areas, intensified development activities have resulted in an increasingly deteriorated living envi-

ronment, which has in turn accelerated global climate change.

Sand and dust aerosol particles are able to produce meaningful climate forcing, either through solar shortwave radiation, or through scattering and absorbing the Earth's long wave radiation. This forcing may affect global weather and climate in a significant manner [3–6]. In this context, SDS (sand and dust storm) activities are able to generate a gradual but far-reaching impact on global climate and environment, in addition to short term severe weather events.

Previous studies showed that a string of countries in the middle and eastern part of East Asia, including Mongolia, China, the Republic of Korea, and Japan, are the victims of

*Corresponding author (email: wjz@cams.cma.gov.cn)

SDS disasters [7]. The development of an SDS system, along with the associated long distance transport of sand and dust, creates an intensified meteorological disaster, not only global but also inter-seasonal [8]. Transitions to the winter and summer seasons are the times when a cold and warm air standoff prevails over the vast mid-latitude area on the northern hemisphere [9].

In recent years, US scientists have tracked long-distance SDS activities in western North America, North Europe, and the Sahara Desert in Africa on a long-term basis, and studied possible approaches to predicting the medium- and long-term SDS processes using integrated methods, including remote sensing and ground observations [10–16].

Meanwhile, Europe and Africa jointly initiated a long-term experiment to predict seasonal SDS events across the Sahara and Arabian deserts. The experiment was carried out in an integrated manner, including observation, diagnosis, and numerical modeling, and produced seasonal and long-term SDS predictions [17]. Apparently, the long-term prediction of SDS activities and associated trends has attracted increased attention from meteorologists.

In recent years, Chinese scientists have achieved great progress in understanding the seasonal and inter-annual variations of sand and dust storms [18–20]. Studies show that the inter-decadal variation of SDS activities and their intensities is associated with the changed behavior of atmospheric circulations in the winter and spring. For example, a year with a raised frequency of SDS activities would have winter and spring climates and atmospheric circulations that are noticeably different from one having fewer SDS occurrences. A year having increased SDS occurrences would show an abnormally deepened vortex in the winter, with a built-up westerly near 50°N, and a northerly polar front in East Asia. Studies also show that inter-annually the frequency of SDS attacks in North China is correlated negatively with the preceding winter's westerly and Arctic Oscillation indexes, but correlated positively with East Asia monsoon indexes in both winter and spring [21].

Based on the SDS concentration data collected by the newly established intensive observing stations, the spatial and temporal distribution data of SDS intensity derived from the FY-2C weather satellite, the data collected by regular stations including 2456 regular weather stations in China, and surface/upper air meteorological data exchanged via the World Meteorological Organization including atmospheric components and NCEP-NCAR reanalysis data, Chinese scientists proposed the concept of the “SDS Footprint Domain” [22, 23]. This is an interesting approach to describing SDS routes based on the observed information, providing evidence for predicting seasonal and long term SDS routes [24].

Previous study [25] indicated that the recent years have witnessed a noticeably increased demand for studying the relationship between atmospheric circulations in the seasonal transition and SDS occurrences and for predicting

SDS intensity trends. Study results [18] show that the polar vortex, a seasonal system, imposes a major impact on shaping the circulations in the transition, especially on the spatial and temporal distribution and the movement of the vortex in the transition from the winter to summer across the Eurasian continent. It regulates cold air activities in East Asia in a significant manner. Study also shows that extensive sea temperature anomalies across the globe create another condition for triggering strong SDS episodes [26].

The SDS disasters caused by the “mutation” of large-scale circulations in the seasonal transition, especially from winter to summer, are not only catastrophic events but also evidence of climate change trends caused by global warming, droughts, and desertification. An SDS event is, more often than not, a suddenly occurring boundary layer meso-scale atmospheric process with disastrous consequences. At the same time, it changes the composition of atmospheric aerosols and their associated evolution, which in turn imposes a slow but far reaching impact on climate [27].

As a result, researchers have begun to work on long-term SDS prediction using cascade discriminant models, and have achieved some progress. For example, Folland and Colman [28] used cluster analysis to make long-term ocean-atmosphere interaction predictions. They made extended predictions based on 500–1000 hPa anomalies. Unfortunately, the complicated calculation of cascade discriminant algorithms and heavy demand for computer resources make the approach unsuitable for actual SDS prediction that may cover a vast region.

In this study, regular meteorological data collected over the period 1980–2006, including surface data, upper air data, and NCEP reanalysis data, were employed. The SDS frequency data applied were from the surface datasets (1980–2006) compiled by the Meteorological Information Center under China Meteorological Administration. A total of 2456 weather stations were selected for data gathering. Meanwhile, the historical SDS frequency records were analyzed, using the original weather charts borrowed from the Meteorological Archive Registry. These charts have covered major areas affected by spring SDS events, including northwest, north, and northeast parts of China, with some SDS processes affecting the lower and middle reaches of the Yangtze River and some areas in South China [22, 24]. Efforts were made to study the 3-D atmospheric circulation structures, and regional, seasonal, and annual differences of SDS activities in the context of spatial and temporal distributions, focusing on the spatial and temporal evolution of large-scale circulations and associated impacts. Meanwhile, the typical and traceable SDS footprints in the seasonal transition were investigated. Genetic probability was employed in the study to establish a cascade discriminant genetic extension model, in an attempt to develop an applicable methodology for predicting the generic long-term trends

of seasonal SDS activities.

1 Analysis of synthesized data

As mentioned above, the significantly altered frequency of SDS attacks is closely associated with the development pattern of polar circulations. As a result, the polar circulation accompanied by a seasonal memory plays a major role in shaping the circulation in the transition from winter to summer, especially in regulating cold air activities across the Eurasian continent. Previous studies show that the phase shift of the Arctic Oscillation index over the past 50 years is associated with SDS activities [29]. In winter (December-February) when the Arctic Oscillation sits in a negative phase, the corresponding zonal circulation index shows a negative anomaly, with a weak westerly at mid-high latitudes appropriate for polar cold air heading south, and a

strong Siberian high pressure. Such a pattern makes North China vulnerable to regional SDS events featuring multiple occurrences. The opposite pattern reduces the probability for a regional SDS event.

In the study, cluster analysis [30] was employed to analyze the relationship between the seasonal/interdecadal variations and the abnormal variations in the polar vortex, in an attempt to develop an approach for evaluating and predicting seasonal and annual SDS intensity.

Figure 1 shows 100 hPa anomalies where SDS weather occurred either in a raised or reduced number during the period 1980–2006. The years 1992, 1995, 1997, 1999, 2001, and 2006 saw more SDS episodes, compared with 1984, 1988, 1989, 2003, and 2005 [24]. Some meaningful patterns can be drawn from Figure 1 as follows:

(1) During a winter preceding fewer SDS occurrences (Figure 1(a)), the upper polar troposphere was noticeably dominated by cyclone circulations, with a negative anomaly

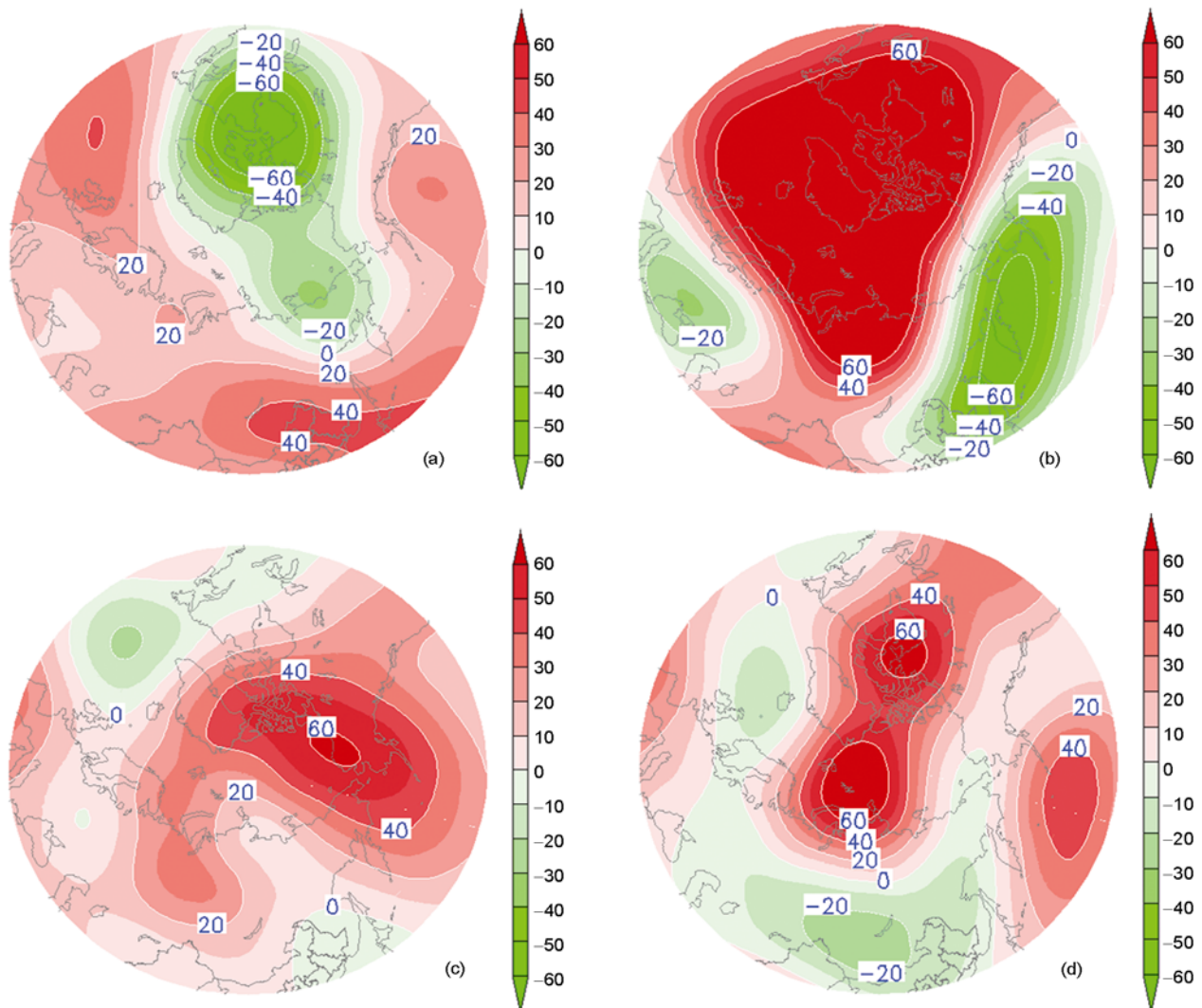


Figure 1 Synthesized 100 hPa anomalies (1980–2006): the preceding winter with less SDS occurrences (a), the preceding winter with more SDS attacks (b), the spring with less SDS occurrences (c), and the spring with more SDS attacks (d). Unit: geopotential meter.

reaching 60 geopotential meters. On the other hand, in a winter preceding more SDS attacks (Figure 1(b)), the upper polar troposphere was noticeably controlled by anti-cyclonic circulations, with a positive anomaly at 80 geopotential meters. The contrasting phase distributions suggest that the preceding winter polar circulation accompanied by an atmospheric memory has an impact on the circulation processes, especially on the intensity of SDS processes across the mid-high latitudes of the northern hemisphere.

(2) In a spring with fewer SDS events, the polar troposphere was noticeably dominated by anti-cyclonic activities, with a raised geopotential from -60 in the preceding winter to more than 60 over a vast region. The Taimyr Peninsula, an area sensitive to cold air activity between the pole and mid-high latitudes on the northern hemisphere, was under the noticeable influence of the “inverse trough” of cyclonic circulations [31], with a raised positive anomaly up to 20 geopotential meters from 0 of the preceding winter (Figure

1(c)). On the other hand, in a spring with raised SDS attacks, the Taimyr Peninsula would have a positive anomaly at 60 or above for upper troposphere circulations (Figure 1(d)). That opposite patterns occur in years with more or fewer SDS events suggests that the polar circulation in the preceding winter is noticeably remembered and has an impact on the intensity of the mid-high latitude circulations and SDS processes in the northern hemisphere.

Figure 2 shows synthesized sea level pressure anomalies for the years with more or fewer SDS events (1980–2006), from which one can extract the following features:

(1) In a winter preceding fewer SDS occurrences (Figure 2(a)), the lower troposphere sea level pressure anomalies sat in a wavy distribution from positive to negative, and to positive again, over an extensive area from the Polar Circle to Northeast Asia, bypassing the northern Pacific Ocean, and ending up near North America. However, in a winter preceding more SDS attacks (Figure 2(b)), a positive-

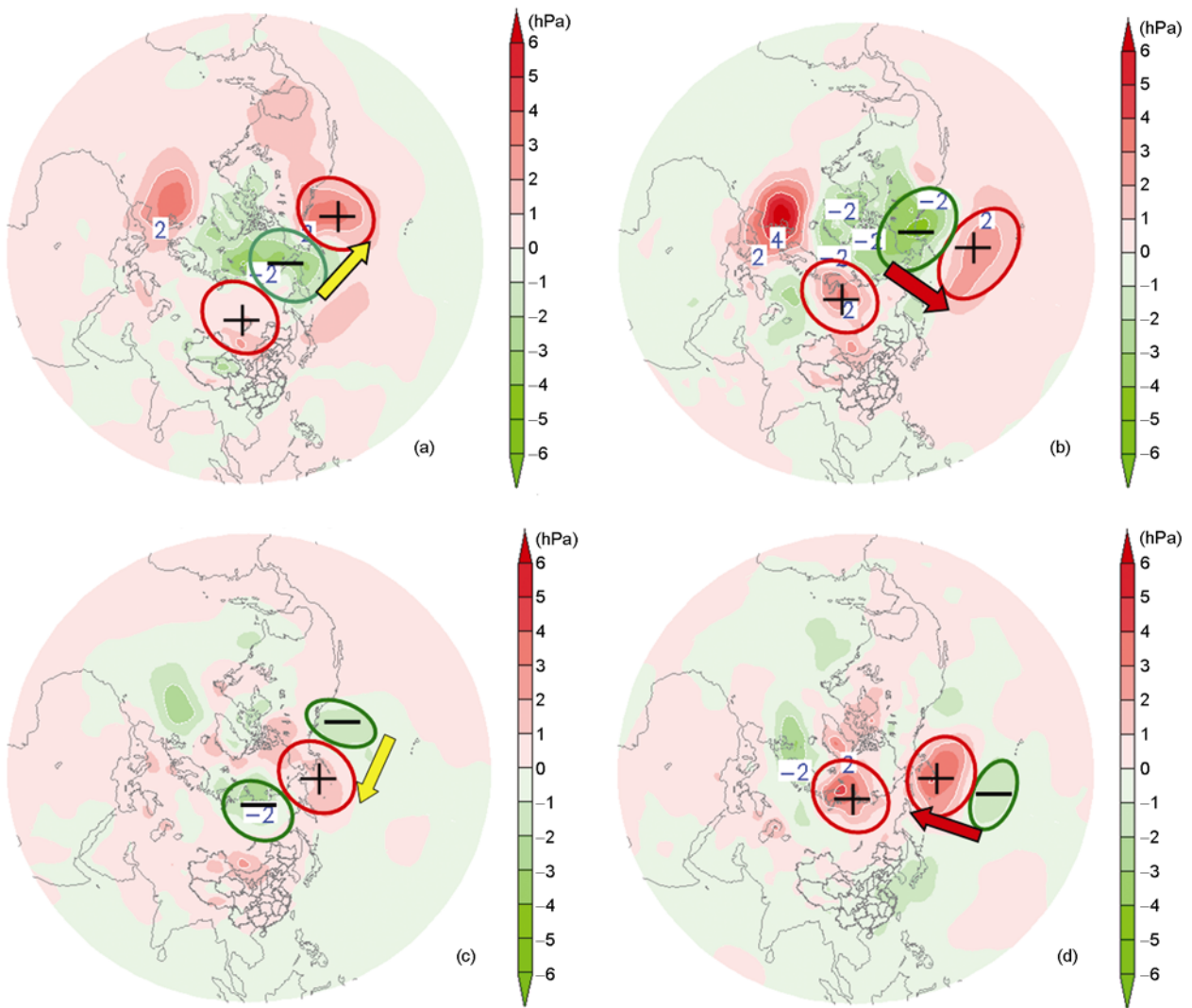


Figure 2 Synthesized sea level pressure anomalies (1980–2006). (a) A winter preceding fewer SDS occurrences; (b) a winter preceding more SDS attacks; (c) a spring with fewer SDS occurrences; (d) a spring with increased SDS occurrences [24].

negative-positive pattern prevailed in the east over a vast area from the Polar Circle to Northeast Asia, further to the northern Pacific Ocean, and ending up near North America, with a heading changed from west-to-east to north-to-south for the negative-positive wave matrix, indicating the forcing of significant sea surface temperature differences from the south to north, and its impact on the distribution of sea level pressure fields.

(2) During the spring shown in Figure 2(c) and (d), significant wavy sea level pressure anomalies prevailed over the above-mentioned regions. However, in a year with fewer SDS occurrences, the wavy anomalies were changed from the positive-negative-positive of the preceding winter to the negative-positive-negative in the spring. In a year with more SDS attacks, anomalies went south from North America to the middle part of the northern Pacific Ocean, with a negative-positive pattern for the preceding winter, and a positive-negative one for the spring.

(3) The above-mentioned footprints indicate that both the polar region and northeast Asia have registered significant wavy anomalies for sea level pressure fields, with a sustained position in the transition from the winter to summer, though the symbols go in opposite directions, implying a significantly mutated polar vortex circulation dominating the Poles and adjacent areas, which has an effect on the intensity and activity of SDS events. This fact has been confirmed by cluster analysis. This agrees with the previous studies [21, 29], which found that the large-scale environment and conditions desirable for SDS occurrences are associated with the abnormal development of sea temperature. Similarly, cluster analysis of mid troposphere circulations (500 and 700 hPa) has revealed a close association between 3-D polar circulations and the frequency of SDS attacks [22]. In the following section, we will discuss the principle and methodology applied in long-term SDS prediction, based on the generic anomalies of 3-D atmospheric circulations over the polar region and mid-high latitudes region in Northeast Asia and the seasonal and annual frequency of SDS attacks.

2 DGAE model

2.1 Basic principles

Folland and Colman [28] employed cluster analysis in preparing long-term sea pressure field prediction, based on a discriminant model. They produced some results on extended long-term prediction of 500–1000 hPa altitude and sea level pressure anomalies [28]. Unfortunately, the complicated calculation and heavy consumption of computer resources makes it undesirable for actual SDS prediction that may cover a vast area. In this context, one has to work out a secondary critical discriminant value y_c to be the initial discriminant predicting seasonal SDS activities. Meanwhile, one has to obtain an extended and refined discriminant spa-

tial and temporal distribution of the geographic (spatial coordinate) and seasonal (temporal coordinate) differences, before establishing a DGAE (Discriminant Genetic Algorithm Extended) model using genetic algorithms.

In the study, efforts were made to sort out the first approximation that reflects the footprints of seasonal and annual SDS activities, through analyzing circulation patterns and observational data, so as to achieve the required discriminant spatial and temporal extension. As the first step, one has to build a discriminant function based on the linear grouping of x_k ($k=1, \dots, P$) as follows:

$$Y_j = \sum_{k=1}^P c_k x_k, \quad (1)$$

where j represents the multi-dimensional discriminant extension, and k the number of x_k , or individual factor number. c_k is a constant coefficient, determined in line with the historical data.

The synthesized analysis made in the preceding part of the paper indicates that the synthesized SDS anomalies are different in geopotential height and sea level pressure both temporally (the preceding winter and following spring) and spatially (the Poles and East Asia). For example, the anomalies in sea level pressure for the winter preceding fewer SDS occurrences (Figure 2(a)) and the winter preceding increased SDS attacks (Figure 2(b)) give opposite symbols (positive and negative) to the spring with fewer SDS occurrences (Figure 2(c)) and the spring having increased SDS attacks (Figure 2(d)) respectively. This provides a clue to seasonal SDS predictions based on the discriminant spatial and temporal distribution. One can work out the corresponding y_j based on the x_k combination, and sort out a discriminant indicator y_c among different y_j values, as an initial prediction. From that, one can further work out discriminant spatial and temporal extension, based on geographic and seasonal differences, achieving a discriminant extension above the spatial and temporal fields (vector).

$$\begin{cases} y_{i(j=1)} = c_{1k}x_{1k} + c_{2k}x_{2k} + c_{3k}x_{3k} \cdots (k=1, 2, 3, \dots, P), \\ y_{i(j=2)} = c_{1k}x_{1k} + c_{2k}x_{2k} + c_{3k}x_{3k} \cdots (k=1, 2, 3, \dots, P), \\ \vdots \\ y_{i(j=m)} = c_{1k}x_{1k} + c_{2k}x_{2k} + c_{3k}x_{3k} \cdots (k=1, 2, 3, \dots, P), \end{cases} \quad (2)$$

where j ($=1, 2, 3, \dots, m$), k ($=1, 2, 3, \dots, P$) mean spatial and temporal vectors respectively. Eq. (2) shows a spatial and temporal vector matrix.

2.2 Secondary critical discriminant

The secondary critical discriminant can be expressed by simplifying eq. (1), using any j in eq. (2): $y=c_1x_1+c_2x_2$. The formula shows an original site through which a plane goes in a 3-D space. Assuming two groups of sites represent two

populations, or group 1 $y \geq y_c$, and group 2 $y < y_c$, then $y = y_c$ makes a discriminant indicator. Then we have population $y > y_c$ and population $y < y_c$. One can deal with them by separating one from the other. For example, when sorting out the cases showing the extreme frequency of SDS attacks using sea level pressure anomaly ΔP (or ΔH , 500 hPa anomaly) and absolute humidity e , one can write eq. (1) as follow:

$$y = c_1 \Delta P + c_2 e.$$

The dispersion defined between the two populations is to be made as large as possible, while the averaged departures \bar{y}_A and \bar{y}_B should not be too far apart. In other words, y in the same population should have a small difference, and the combination of the two populations is to meet the following formula:

$$\frac{\partial}{\partial C_k} \left[\frac{(\bar{y}_A - \bar{y}_B)^2}{\sum_{i=1}^{N_1} (y_{Ai} - \bar{y}_A)^2 + \sum_{i=1}^{N_2} (y_{Bi} - \bar{y}_B)^2} \right] = 0, \quad (k=1, \dots, P).$$

Then, one can have the following:

$$\begin{cases} S_{11}C_1 + S_{12}C_2 + \dots + S_{1P}C_P = \bar{x}_1(A) - \bar{x}_2(B), \\ S_{21}C_1 + S_{22}C_2 + \dots + S_{2P}C_P = \bar{x}_1(A) - \bar{x}_2(B), \\ \vdots \\ S_{P1}C_1 + S_{P2}C_2 + \dots + S_{PP}C_P = \bar{x}_P(A) - \bar{x}_P(B), \end{cases} \quad (3)$$

where S stands for the correlation between different forecast factors. One can work out C_1, C_2, \dots, C_P using the eq. (2), when expressing matrix space ($j=1, m$), will have the following form:

$$y = \sum_{k=1}^P C_k x_k, \quad \bar{y}(A) = \sum_{k=1}^P C_k \bar{x}_k(A), \quad \bar{y}(B) = \sum_{k=1}^P C_k \bar{x}_k(B).$$

Prediction evidence can be obtained from the following:

$$y_c = [N_1 \bar{y}(A) + N_2 \bar{y}(B)] / (N_1 + N_2), \quad (4)$$

where N_1 and N_2 are the number of samples in each population. When $\bar{y}(A) > \bar{y}(B)$ is established, $y > y_c$ would bring out prediction A, and $y < y_c$ prediction B, or vice versa, namely in the case of $\bar{y}(A) < \bar{y}(B)$, $y > y_c$ would result in prediction B, and $y < y_c$, prediction A.

2.3 Discriminant genetic extension

Cochran and Bliss [32] were the first group of scientists to propose dealing with complicated events using discriminant

spatial and temporal vector analysis. The methodology was employed by Miller [33] in the discriminant prediction of meteorological elements, including rain, snow, freezing rain, and sleet, with applications in the early part of results. The complicated calculation program forced people to use simplified two-tiered discriminant algorithms, rather than the cascade discriminant system [34]. In recent years, the discriminant theory has found more applications in computer graphics and weather forecasting [35]. Australian scientist Keenan [36] introduced decision making rules in preparing typhoon track forecasts, and used the strategy of linear discriminant functions to realize the extension, with secondary discriminant prediction results being derived from the above-mentioned eqs. (1)–(4), where eq. (1) becomes:

$$y_j = \sum_{k=1}^P c_{kj} x_k.$$

The calculation was further extended to the spatial and temporal vector matrix, allowing x_k to become the spatial distribution of sensitive elements obtained through the synthesized analysis of inter-seasonal footprints of SDS activities [37]:

$$X^{(j)} = (X^{(1)}, X^{(2)}, \dots, X^{(n)}), \quad (5)$$

where $X^{(1)}, X^{(2)}, \dots, X^{(n)}$ are the anomalies of sensitive elements derived from the synthesized analysis and sea level pressure anomalies at 200, 500, and 700 hPa respectively. Keenan [36] made typhoon movement track forecasts by dividing the extension into a number of j populations, in an attempt to obtain the required posterior probability:

$$P_j = q_j \exp y_j / \sum_{k=1}^P q_g \exp y_g, \quad (q=1, 2, 3, \dots, G), \quad (6)$$

where, q_j represents the prior probability of No. j population, or a condition free probability in No. j population. P_j is the posterior probability of No. j population. In other words, assuming y_j is there, the size of different P_j is compared, before making the forecast based on the population having the largest probability. Experiments show that the length of time required and problems with stability make the calculation undesirable for extensive or large-scale predictions. In this study, genetic probability was used as a substitute for posterior probability. Unfortunately, it also had the problem of probability mutation in the extension process. Assuming the largest probability mutation is P_{m0} , and the smallest one P_{m1} , the genetic probability can be expressed as follows [38]:

$$P_m = P_{m0} \exp \left[- \left(\frac{f_{\max} - \bar{f}}{\sigma_1} \right) \right], \quad (7)$$

$$\sigma_1 = \frac{10f}{\sqrt{\ln P_{m0} - \ln P_{m1}}}, \quad (8)$$

where f means a larger adaptability of crossover inheritance, f_{\max} the largest adaptability, and \bar{f} the population averaged adaptability. f , a genetic selective adaptability function, is expressed as [39]:

$$f_i = \frac{(1-\mu)^{i-1}}{\mu}. \quad (9)$$

Both crossover inheritance and mutation are the strengths of genetic algorithms. The extension with GA can expect both the continuation of the historical evolution and possible mutations. In eq. (9), i can be calculated based on historical observational data, and $\mu \in (0, 1)$ is a constant [38]. Now one can calculate the genetic probability of corresponding SDS episodes in the past: P_m ($m=1, 2, 3, \dots, G$), and obtain the spatial distribution of the largest adaptability, by comparing the size of different populations. The population having the largest probability defines the forecast fields, which makes discriminant genetic extension possible.

3 Experimental forecasts

The DGAE model established in the study to predict seasonal SDS activities over a given region was employed to predict the frequency of spring SDS activities occurring in North China over the period 2007–2009. Experimental forecasts have provided high resolution regional distributions of SDS processes, a meaningful reference for long-term SDS prediction in the future.

Figure 3 shows the results of regional SDS process pre-

diction for the spring of 2009. For the convenience of viewing, the gray legend has been turned into anomaly percentages. The red color area (positive) shows the multi-year averaged positive anomaly, and the blue color area (negative) the multi-year averaged negative anomaly. One can see in Figure 3 that for a number of regions, including most of northern China, the southern part of northeastern China, and the southern part of the Korean Peninsula, a low frequency of SDS attacks in the spring is predicted. Of the regions mentioned, the Songliao Plains in northeastern China was predicted to have the lowest frequency of SDS attacks. The northwestern part of the country saw a significant positive departure, with the largest positive departure appearing in the western part of Gansu, Ningxia, and the northern part of Shaanxi. Experimental results show that the DGAE model established in the study is able to produce an objective and refined discriminant prediction capability that can be used to tell the differing intensities and regional distributions of seasonal SDS events in China.

4 Conclusion and discussion

The study has resulted in the following preliminary findings:

(1) The paper discusses the diagnostic and discriminant footprints of 3-D atmospheric circulation structures and the spatial and temporal distributions of regional, seasonal, and annual SDS activities. It also makes genetic probability a substitute for posterior probability, and develops a DGAE model to predict the seasonal footprints of regional SDS activities in East Asia.

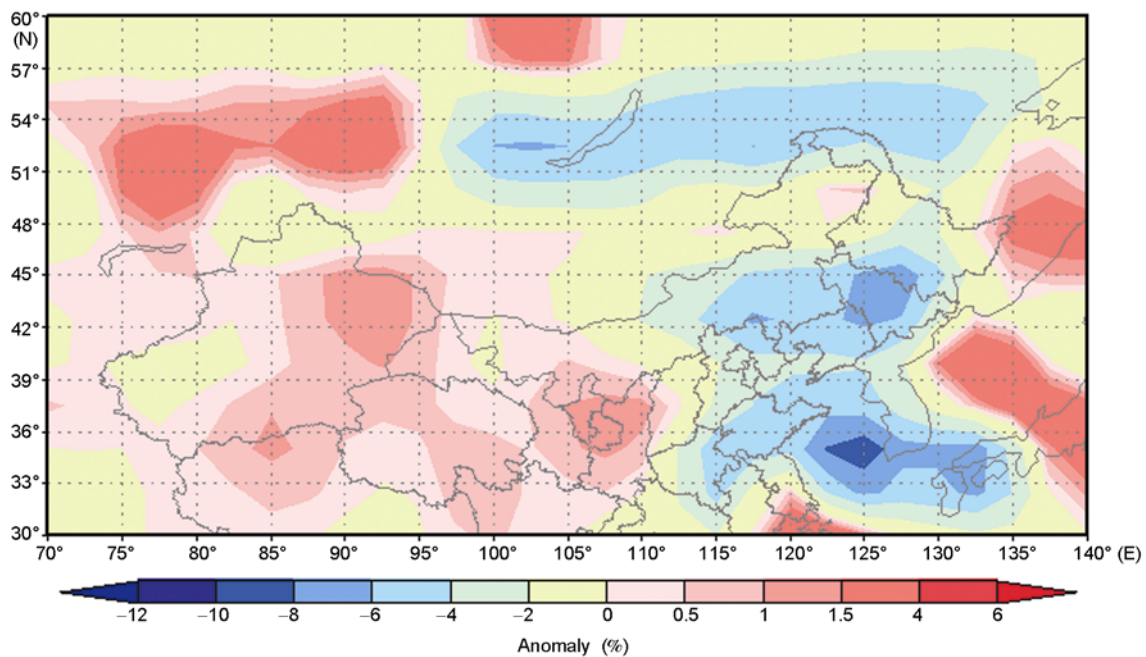


Figure 3 Distribution of regional SDS processes predicted by DGAE-SDS model for the spring of 2009.

(2) Synthesized discriminant SDS analysis shows that the polar circulation in the preceding winter has a noticeable memory of and an impact on the intensity of mid-high latitude circulations and regional SDS processes on the northern hemisphere. The polar circulation, a seasonal system, plays a major role in regulating the circulations in the seasonal transition.

(3) Based on the diagnostic and discriminant understanding of 3-D atmospheric circulation structures and the spatial and temporal distribution of regional, seasonal, and annual SDS activities, secondary critical discriminant values have been worked out to be the first approximation to the initial discriminant prediction. Genetic algorithms are introduced, where genetic probability is used as a substitute for posterior probability, in an attempt to show the dual characteristics of crossover inheritance and mutation and build a non-linear adaptability function for genetic algorithm extension. This reveals the spatial distribution of the largest adaptability for defining the forecast field, making discriminant genetic extension possible. This effort has led to the establishment of a regional model for predicting seasonal SDS activities in East Asia. The model was tested to predict the spring SDS activities occurring in North China over the period from 2007 to 2009. The experiment has produced high resolution intensity ratings and regional distributions of SDS activities, providing a meaningful reference for seasonal SDS predictions in the future.

Previous studies show that complicated calculation and heavy time consumption have made the traditional cascade discriminant analysis unsuitable for extensive or large-scale predictions. The model established by this study makes genetic probability a substitute for posterior probability, showing the dual characteristics of crossover inheritance and mutation and developing a non-linear adaptability function for genetic extension. This reveals the spatial distribution of the largest adaptability, making discriminant genetic extension possible by producing the forecast field that agrees with the population having the largest genetic probability.

The DGAE model developed in the study can be used to predict seasonal SDS activities, though it is a preliminary attempt at establishing an applicable model for predicting seasonal SDS activities in East Asia. The model, however, will contribute to the improvement of long-term SDS prediction.

We thank Prof. Zhang Xiaoye of the Chinese Academy of Meteorological Sciences and Prof. Gong Sunling of the Air Quality Research Division, Science & Technology Branch, Environment Canada for their valuable suggestions and discussion. The study was supported by National S & T Support Program (Grant No. 2008BAC40B02), National Basic Research Program of China (Grant Nos. 2006CB403703 and 2006CB403701), and Basic Research Fund under Chinese Academy of Meteorological Sciences (Grant Nos. 2009Y002, 2009Y001).

- 1 Zhang Q, Gao G, Wang M, et al. Monitoring and early warning services for spatial and temporal changes of droughts and floods in China in recent 50 years (in Chinese). 200 Years Annual Meeting of Chinese Meteorological Society. Beijing: China Meteorological Press, 2004. 383–384
- 2 Li C Y. Introduction to Dynamic Climate (in Chinese). Beijing: China Meteorological Press, 1995. 1–4
- 3 Ding J, Zhu T. Heterogeneous reactions on the surface of fine particles in the atmosphere. *Chin Sci Bull*, 2003, 48: 2267–2276
- 4 Shi G Y, Zhao S X. On the scientific problems of sandstorm study (in Chinese). *Chin J Atmos Sci*, 2003, 27: 591–606
- 5 Shen S H, Chen S J. Numerical simulation for frontogenesis process due to radiation forcing of sand storms (in Chinese). *Acta Meteorol Sin*, 2003, 27: 591–606
- 6 Wang S G, Yang D B, Jin T, et al. Black storm in Northwest China causes and countermeasures (in Chinese). *J Desert Res*, 1995, 15: 19–30
- 7 Zhang X Y. Spring Sandstorms in Northeast Asia in 2006 (in Chinese). Beijing: China Meteorological Press, 2006. 9–19
- 8 Thompson D W J, Wallace J M. The Arctic Oscillation signature in the wintertime geo-potential height and temperature fields. *Geophys Res Lett*, 1998, 25: 1297–1300
- 9 He C, He J H. The relationship between the northern polar oscillation and temperature variations in winter (in Chinese). *J Nanjing Instit Meteorol*, 2003, 26: 1–7
- 10 Swap R. Dust in the Amazon Basin. *Tellus*, 1992, 44B: 133–149
- 11 Franzen L G. The Saharan dust episode of southern and central Europe, and northern Scandinavia March, 1991. *Weather*, 1995, 50: 313–318
- 12 Genthon C. Simulations of desert dust and sea-salt aerosols in Antarctica with a general circulation model of the atmosphere. *Tellus Ser B-Chem Phys Meteorol*, 1992, 44: 371–389
- 13 Joseph P V, Raipal D K, Deka S N, et al. The convective dust storms of Northwest India. *Mausam*, 1980, 31: 431–442
- 14 Wolfson N, Marson M. Satellite 1986: Observations of a phantom the desert. *Weather*, 1986, 41: 57–60
- 15 Iwasaka Y. The transport and spatial scale of Asian dust-storm clouds: A case study of the dust-storm event of April, 1979. *Tellus Ser B-Chem Phys Meteorol*, 1983, 35: 189–196
- 16 Ellis J R, W G, Merrill J T. Trajectories for Saharan dust transported to Barbados using Stokes's law to describe gravitational settling. *J Applied Meteorol*, 1995, 34: 1716–1726
- 17 Cuevas E, Baldasano J M, Pérez C, et al. The SDS-GEOEurope GEO-System oriented System. International Sand and Dust Storm Warning System. Barcelona: WMO/GEO Expert Meeting, 2007. 7–9
- 18 Gao Q X, Su F Q, Ren Z H, et al. Sandstorms in Beijing and its impact (in Chinese). *China Environment*, 2002, 32: 468–471
- 19 Zhang S L, Gong S L, Shen Z X, et al. Characterization of soil dust aerosol in China and its transport and distribution during 2003 ACE-Asia. *J Geophys Res*, 2003, 108(D9): 4261, doi: 10.1029/2002JD002632
- 20 Ye D Z, Chou J F, Liu J Y. A study on the causes of sandstorms in northern China and its countermeasures (in Chinese). *Acta Geograph Sin*, 2000, 55: 513–521
- 21 Kang D J, Wang H J. Analysis on the decadal scale variation of the dust storm in North China. *Sci China Ser D-Earth Sci*, 2005, 48: 2260–2266
- 22 Yang Y Q, Hou Q, Zhou C H, et al. Sand/dust storm processes in Northeast Asia and associated large-scale circulations. *Atmos Chem Phys*, 2008, 8: 25–33
- 23 Wang Y Q, Zhang X Y. The contribution from distant dust spruces to the atmospheric particulate matter loading at Xi'an, China during spring. *Sci Total Environment*, 2006, 368: 875–883
- 24 Wang J Z, Yang Y Q, Zhou C H, et al. A study on weather process characteristics of spring SDS in 1980–2007. In: Fifth International Workshop on Sand and Dust Storms (SDS). Beijing: Meteorology Press, 2008. 9–11
- 25 Sun J, Li Z C. A Preliminary study on Sandstorms forecast method in

- the northwest of Chin (in Chinese). *Meteorol Monthly*, 2001, 27: 19–24
- 26 Fan K, Wang H J. Interannual variability of Antarctic Oscillation and its influence on East Asian climate during boreal winter and spring. *Sci China Ser D-Earth Sci*, 2006, 49: 554–560
- 27 Gong S L, Barrie L A, Blanchet J P, et al. Canadian aerosol module: A size-segregated simulation of atmospheric aerosol processes for climate and air quality models 1. Module development. *J Geophys Res*, 108(D1): 4007, doi: 10.1029/20012003JD002002
- 28 Folland C K, Colman A. A multivariate technique for use in long-range forecasting. *Programme Long-range Forecasting WMO/TD*, 1985, 87: 628–636
- 29 Song L C, Yu Y X, Sun X Y, et al. Relationship between Arctic Oscillation and strong sandstorm in the North of China (in Chinese). *Plateau Meteorol*, 2004, 23: 835–839
- 30 Li Y, Wang J Z, Chen L S, et al. Study on rainfall distribution associated with typhoon Matsa (2005). *Chin Sci Bull*, 2007, 52: 972–983
- 31 Gao S T, Tao S Y, Ding Y H. Interaction between upper air waves and East Asia jet during cold wave (in Chinese). *Chin J Atmos Sci*, 1992, 16: 718–724
- 32 Cochran W G, Bliss C I. Discriminant function with covariance. *Ann Math Statist*, 1948, 19: 151–176
- 33 Miller R G. Statistical prediction by discriminant analysis. *Meteorol Monmg*, 1962, 4: 1–15
- 34 Suzuki E. Categorical prediction schemes of rainfall types by discriminant analysis. *Papers Meteorol Geophys*, 1964, 15: 119–160
- 35 Wang J Z, Yang Y Q. *Modern Weather Engineering* (in Chinese). Beijing: China Meteorological Press, 2000. 334–339
- 36 Keenan T D. Forecasting tropical cyclone motion using a discriminant analysis procedure. *Mon Rev*, 1986, 144: 434–441
- 37 Yang Y Q, Hou Q, Wang J Z. A study on prediction of SDS annual, tendency and operational testing. In: *Fifth International Workshop on Sand and Dust Storms (SDS)*. Beijing: Meteorology Press, 2008. 21–24
- 38 Yang Y Q, Wang J Z. An integrated decision method for prediction of tropical cyclone movement by using genetic algorithm. *Sci China Ser D-Earth Sci*, 2005, 48: 429–440
- 39 Li Q L, Xu X F. A self-adaptive genetic algorithm for partner selection of agile virtual enterprise (in Chinese). *Infor Adv Techn*, 2001, 10: 66–69